Cancer Research

PLAC8 Localizes to the Inner Plasma Membrane of Pancreatic Cancer Cells and Regulates Cell Growth and Disease Progression through Critical Cell-Cycle Regulatory Pathways

Brajesh P. Kaistha[1], Holger Lorenz[2], Harald Schmidt[1], Bence Sipos[3], Michael Pawlak[4], Berthold Gierke[4], Ramona Kreider[1], Brigitte Lankat-Buttgereit[1], Melanie Sauer[1], Lisa Fiedler[1], Anja Krattenmacher[1], Bettina Geisel[1], Johann M. Kraus[5], Kristopher K. Frese[6], Sabine Kelkenberg[7], Nathalia A. Giese[8], Hans A. Kestler[5], Thomas M. Gress[1], and Malte Buchholz[1]

Abstract

Pancreatic ductal adenocarcinoma (PDAC) carries the most dismal prognosis of all solid tumors and is generally strongly resistant to currently available chemo- and/or radiotherapy regimens, including targeted molecular therapies. Therefore, unraveling the molecular mechanisms underlying the aggressive behavior of pancreatic cancer is a necessary prerequisite for the development of novel therapeutic approaches. We previously identified the protein placenta-specific 8 (PLAC8, onzin) in a genome-wide search for target genes associated with pancreatic tumor progression and demonstrated that PLAC8 is strongly ectopically expressed in advanced preneoplastic lesions and invasive human PDAC. However, the molecular function of PLAC8 remained unclear, and accumulating evidence suggested its role is highly dependent on cellular and physiologic context. Here, we demonstrate that in contrast to other cellular systems, PLAC8 protein localizes to the inner face of the plasma membrane in pancreatic cancer cells, where it interacts with specific membranous structures in a temporally and spatially stable manner. Inhibition of PLAC8 expression strongly inhibited pancreatic cancer cell growth by attenuating cell-cycle progression, which was associated with transcriptional and/or posttranslational modification of the central cell-cycle regulators CDKN1A, retinoblastoma protein, and cyclin D1 (CCND1), but did not impact autophagy. Moreover, Plac8 deficiency significantly inhibited tumor formation in genetically engineered mouse models of pancreatic cancer. Together, our findings establish PLAC8 as a central mediator of tumor progression in PDAC and as a promising candidate gene for diagnostic and therapeutic targeting. *Cancer Res; 76(1); 96–107. ©2015 AACR.*

Introduction

Pancreatic ductal adenocarcinoma (PDAC) continues to be one of the most lethal forms of cancer. With 5-year survival rates below of 6% and median survival times of approximately 6 months after diagnosis, PDAC carries the most dismal prognosis of all solid tumors (1). Surgical resection of early stage tumors potentially offers a chance to cure the disease, but is hindered by the fact that the vast majority of tumors is not detected until already in an advanced regional (27%) or distant (53%) stage (1). In addition to the late presentation, patient prognosis is worsened by the fact that PDAC shows extreme resistance to currently available chemo- and/or radiotherapy regimens (2). There is thus a continuing and pressing need to unravel the molecular mechanisms underlying the extremely aggressive biology of PDAC tumors in order to provide a basis for the development of novel concepts to battle this disease.

In previous genome-wide mRNA expression analyses of microdissected human pancreatic tissues, we have identified ectopic expression of the mRNA encoding the protein placenta-specific 8 (PLAC8) in advanced preneoplastic lesions [pancreatic intraepithelial neoplasia grade 3 (PanIN3)] and invasive PDAC (3). PLAC8, also known as onzin, is a small protein (~16 kDa) that was originally described to be highly expressed in mouse placenta (4, 5). PLAC8 mRNA expression has subsequently also been detected in myeloid and lymphoid cells as well as lung and intestinal epithelial cells (6). Plac8 deficiency in mice has been described to result in defects in innate immunity (6), impaired

[1]Clinic for Gastroenterology, Endocrinology, Metabolism and Infectiology, Philipps-University Marburg, Marburg, Germany. [2]Central Imaging Facility, Zentrum für Molekulare Biologie der Universität Heidelberg (ZMBH), Heidelberg, Germany. [3]Department of Pathology, University Clinic Tübingen, Tübingen, Germany. [4]Department of Biochemistry and Protein Profiling, NMI Natural and Medical Sciences Institute at the University of Tübingen, Reutlingen, Germany. [5]Medical Systems Biology, University of Ulm, Ulm, Germany. [6]Princess Margaret Hospital, University of Toronto, Toronto, Canada. [7]CeGaT GmbH, Tübingen, Germany. [8]Department of Surgery, University Clinic Heidelberg, Heidelberg, Germany.

Note: Supplementary data for this article are available at Cancer Research Online (http://cancerres.aacrjournals.org/).

T.M. Gress and M. Buchholz share equal authorship.

Corresponding Author: Malte Buchholz, University of Marburg, Zentrum für Tumor- und Immunbiologie, Hans-Meerwein-Str. 3, Marburg 35043, Germany. Phone: 49-6421-2821435; Fax: 49-6421-2821432; E-mail: malte.buchholz@staff.uni-marburg.de

doi: 10.1158/0008-5472.CAN-15-0216

brown and white fat differentiation as well as late onset obesity (7, 8), and contact hypersensitivity (9). Although evolutionarily highly conserved, the protein does not contain any known functional domains, and its molecular function remains enigmatic. Moreover, the cellular role of PLAC8 seems to be highly context-dependent, resulting in strongly variable, and sometimes contradictory, effects of PLAC8 modulation in different cell types, ranging from apoptosis protection in fibroblasts (10) versus apoptosis induction in human lymphocytes (11) to inhibition of cell differentiation in primary acute myeloid leukemia cells (12), and induction of epithelial-to-mesenchymal transition in cultured colon cancer cells (13).

We demonstrate here that, contrary to other cellular systems, the PLAC8 protein primarily localizes to the inner face of the plasma membrane in pancreatic cancer cells, where it interacts with specific membranous structures in a temporally and spatially stable manner. Inhibition of PLAC8 expression strongly inhibited pancreatic cancer cell growth by attenuating cell-cycle progression, which was associated with transcriptional and/or posttranslational modification of the central cell-cycle regulators p21 (CDKN1A), retinoblastoma protein (RB1) and cyclin D1 (CCND1), while autophagy was not impacted. Moreover, PLAC8 deficiency significantly inhibited tumor formation in Kras–driven, but not Kras/Trp53–driven genetically engineered mouse models (GEMM) of pancreatic cancer. PLAC8 thus appears to be a central regulator of tumor progression in PDAC and represents a promising novel gene for diagnostic and therapeutic targeting.

Materials and Methods

Cell lines, patient samples, and tissue microarrays

Panc-1 (14) and HEK-293 (15) cells were obtained from the American Type Culture Collection. S2-007 and S2-028 were from T. Iwamura (16; Miyazaki Medical College, Miyazaki, Japan). IMIM-PC1 and IMIM-PC2 cells were kindly provided by F.X. Real (17; CNIO, Madrid, Spain). PaTu-8988T and PaTu-8988S cells were kindly provided by H.P. Elsässer (Cytobiology and Cytopathology Institute, Philipps University, Marburg, Germany). These cell lines were maintained in Dulbecco's modified minimal essential medium (Gibco) supplemented with 10% FCS (PAA) and cultured at 37°C/5% CO_2.

Immortalized human pancreatic ductal cells (HPDE; ref. 18) were cultured in defined keratinocyte serum-free medium supplemented with human recombinant epidermal growth factor and bovine pituitary extract (Gibco/Life Technologies).

Cancer cell line identities were verified using the GenomeLab Human STR Primer Set (Beckman Coulter) on a CEQ8800 sequencer (Beckman Coulter) according to the manufacturer's protocol. STR data were submitted to online verification tool of DSMZ (www.dsmz.de) to confirm the identity of human cell lines.

Surgically resected PDAC and chronic pancreatitis (CP) tissues samples were procured from the surgery departments of the University of Heidelberg and Ludwig Maximilian University of Munich. Samples of normal pancreatic tissue were obtained from the healthy donors. Informed consent in writing was obtained from all patients prior to using tissue samples. The study was approved by the ethics committee at the University of Heidelberg and Ludwig Maximilian University of Munich, Germany.

For construction of tissue microarrays (TMA), 1 mm (tumor) and 1.5 mm (normal tissue) sized tissue biopsies were extracted from paraffin donor blocks and transferred into prepunched holes on recipient paraffin blocks with a tissue microarrayer (Beecher Instruments, Inc.) equipped with a TMA booster (Alphelys). The recipient blocks were sealed for 10 minutes at 56°C and 30 minutes at 4°C. This procedure was repeated twice. The TMA blocks were cut into 3.5 μm sections and placed on SuperFrost Plus slides for immunohistochemical staining.

Immunohistochemical staining was performed with a rabbit polyclonal anti-PLAC8 antibody (Sigma-Aldrich, cat. # HPA040465; 1:100 dilution) on the Ventana BenchMark XT system (Ventana Medical Systems) including the deparaffinization of the formalin-fixed paraffin-embedded tissue sections and the heat-induced antigen-retrieval. The intensity of the reactions was scored as mild, moderate, or strong (score 1, 2, or 3, respectively). The proportion of the positive cells in ducts and tumor areas was estimated in percent and divided into scores (<10% = 1, 10%–50% = 2, 51%–80% = 3, >80% = 4). The final score was determined as a product of the intensity of the staining and the proportion of positive cells (minimum 0, maximum 12).

PLAC8 expression constructs

The full-length *PLAC8* open reading frame (ORF) was purchased from Open Biosystems, PCR-amplified using specific primers and cloned into the pENTR vector (Invitrogen/Life Technologies). The ORF was then shuttled into the pdECFP and pdEYFP expression vectors (19) using the Gateway cloning system (Invitrogen/Life Technologies), producing an N-terminal fusion construct with cyan fluorescent protein (CFP) as well as a C-terminal fusion construct with yellow fluorescent protein (YFP).

Functional microscopy

The plasmid pEYFP-N1 was from Clontech. The plasmids pssRFP-KDEL, pcGFP-wtPrP, and pMyrPalm-mEYFP (20–22) have been described previously. Anti-GFP antibody reacts to all GFP-derived fluorescent proteins and has been described previously (23).

Transient transfections were performed using 25 kDa linear polyethylenimine (Polysciences). Wide-field fluorescence images were acquired with a CellR IX81 microscope system (Olympus) using an UPLSAPO ×60 1.35 numerical aperture (NA) oil objective lens and appropriate filter settings. For total internal reflection fluorescence (TIRF) imaging an Olympus IX81 CellTIRF microscope equipped with a 100×1.4 NA oil objective lens (Olympus) and an ImagEM (C9100-13) camera (Hamamatsu) was used. PLAC8-YFP fluorescence was excited with a 50 mW 488 nm diode laser (Olympus). Confocal imaging was performed with a Zeiss LSM 780 microscope and pinhole settings between 1 and 3 airy units. CFP, GFP, and YFP fluorescence was excited with the argon laser and RFP fluorescence was excited with a 561 nm diode-pump solid-state laser. PLAC8 signal quantification was measured using an LSM 780 confocal microscope from Zeiss. Very thin confocal slices (pinhole 0.76) of transiently transfected S2-007 cells were used for the analysis 22 to 24 hours after transfection. Regions of interest covering background (untransfected cells), cytosol, and membrane localizations were defined and signal intensities measured in $n = 12$ independent cells from $n = 3$ replicate experiments (arbitrary units).

The application, methodology, and a detailed protocol of the fluorescence protease protection assay have been described previously (24, 25). In brief, cells were first permeabilized with 20 μmol/L digitonin in KHM buffer (110 mmol/L potassium

acetate, 20 mmol/L HEPES, 2 mmol/L $MgCl_2$), then washed with KHM buffer to remove digitonin and finally treated with 4 mmol/L trypsin in KHM buffer for the indicated time.

Fluorescence recovery after photobleaching (FRAP) and fluorescence loss in photobleaching (FLIP) measurements (26) were performed on a LSM780 confocal microscope using a ×63 1.4 NA oil Plan-Apochromat objective (Zeiss). Cells were grown on 8-well μ-slides (ibidi GmbH) and subjected to FRAP or FLIP analyses at 37°C for no longer than 2 hours. For quantitative FRAP analyses, recovery curves and values for the halftime of fluorescence recovery and mobile fraction were derived from 10 cells investigated for each condition. The mobile fraction was calculated by comparing the photobleach corrected prebleach and postbleach recovery fluorescence intensity values in the photobleached region of interest (ROI) as described previously (27). Image processing and analysis was performed using ImageJ (28).

siRNA transfection of cell lines

Pancreatic cancer cell lines were transfected with siRNAs using siLentFect Lipid Reagent (Bio-Rad) according to the manufacturer's protocol. Unless stated otherwise, for transfection 1.5×10^5 cells were seeded per well in a 6-well plate. Three Silencer Select siRNAs (Life Technologies, cat. # 16708) targeting the *PLAC8* ORF were used: ID24641, ID24734, and ID46267 (designated si1, si2, and si3 in the article, respectively). In addition, c-Myc-specific siRNAs with IDs 106820 and 114231 were used. Accell Control siRNA #1 (Thermo Scientific-Dharmacon) was used as a nonsilencing control.

RNA extraction, cDNA synthesis, and qRT-PCR

RNA from cell lines was extracted using peqGold Total RNA Kit (PEQLAB GmbH) according to the manufacturer's protocol. Tissue samples were homogenized in liquid nitrogen using a mortar and pestle and RNA extracted using the RNeasy Mini Kit (Qiagen) following the manufacturer's protocol. One microgram of total RNA was used for first-strand cDNA synthesis using the Omniscript RT Kit (Qiagen) as per the manufacturer's protocol. Quantitative real-time reverse transcription PCR (qRT-PCR) was performed using SYBR Green MasterMix (Applied Biosystems) on a 7500 Fast Realtime PCR system (Applied Biosystems). The following primer pairs were used for qRT-PCR:

ribosomal protein, large, P0; RPLP0_For: 5′-TGGGCAAGAACACCATGATG-3′; RPLP0_Rev: 5′-AGTTTCTCCAGAGCTGGGTTGT-3′; hPlac8_For: 5′-GGGTGTCAAGTTGCAGCTGAT-3′; hPlac8_Rev: 5′-TAGATCCAGGGATGCCATATCG-3′; mPlac8_For: 5′-GGCTCAGGCACCAACAGTTAT-3′; mPlac8_Rev: 5′-GCAGTCACTGAAGCAATCACACA-3′.

Reverse phase protein array analyses

Reverse phase protein array (RPPA) technology was used for high-content analysis of signaling proteins (expression and post-translational modifications) as described earlier (29). S2-007 cells (transfected with PLAC8-specific siRNAs 1–3, nonsilencing control siRNA or left untreated) were prepared as three biologic replicates (15 samples in total). Whole cell lysates were produced by incubating treated and washed cell cultures *in situ* with 200 μL of denaturing lysis buffer CLB1 (Zeptosens/Bayer Technology Services GmbH) for 30 minutes at room temperature. Protein concentrations of the lysate supernatants were determined by Bradford Assay (Coomassie Plus, Thermo Scientific). For production of RPPA, cell lysates were adjusted to 3 mg/mL protein concentration in CLB1 buffer and subsequently diluted 10-fold with printing buffer CSBL1 (Zeptosens). The lysates were printed as duplicate spots onto Zeptosens chips using a Gesim NP2.0 Nanoplotter (GeSiM) and single-droplet deposition of lysate (0.4 nL per sample spot). After assay measurements (one protein per array), array images and data were analyzed with the software ZeptoVIEW 3.1 (Zeptosens).

Protein extraction and Western blotting

For protein extraction, cells were collected together with medium and centrifuged at 1,600 rpm at 4°C for 5 minutes. Pellets were washed twice with ice-cold PBS and then resuspended in 200 μL lysis buffer (PBS containing protease inhibitors (Protease Arrest, GBiosciences) and phosphatase inhibitors (PMSF 1 mmol/L, EDTA 0.5 mmol/L, sodium pyrophosphate 25 mmol/L, sodium orthovanadate, 10 mmol/L, sodium fluoride 50 mmol/L)). Cells were sonicated (LabSonic, BBraun) and protein content was assessed using Protein Assay Reagent (Thermo Scientific). For Western blotting, 10 μg proteins were electrophoresed on SDS-polyacrylamide gels and electrophoretically transferred onto nitrocellulose membranes (Optitran, GE Healthcare Life Sciences). Membranes were blocked in 5% nonfat dry milk in TBST (10 mmol/L Tris–HCl, pH 7.6, 100 mmol/L NaCl, 0.1% Tween 20) for 2 to 4 hours at room temperature and then probed with appropriate primary and secondary antibodies: anti–Phospho-Rb (Ser807/811): Cell Signaling, cat. # 9308; anti–Phospho-S6-ribosomal protein (Ser235/236): Cell Signaling, cat. # 2211; anti–Cyclin D1: Abcam, cat. # ab16663; anti-PLAC8: Sigma-Aldrich, cat. # HPA040465; anti-p21: Cell Signaling, cat. # 2947; anti-PARP: Cell Signaling, cat. # 9532; anti–caspase-3: Cell Signaling, cat. # 9664 and 9665; anti-LC3A/B: Cell Signaling, cat. # 12741 and anti–actin-HRP coupled: Sigma-Aldrich, cat. # A3854; anti–c-Myc: Cell Signaling, cat. #9402; anti-Akt: Cell Signaling, cat. #9272; anti–Phospho-Akt: Cell Signaling, cat. #3787.

Proliferation and viability assays

For BrdUrd incorporation assays using the Cell Proliferation ELISA Kit (Roche Diagnostics), 5,000 to 7,500 cells were reseeded 24 hours after transfection into a ViewPlate-96 Black cell culture plate (PerkinElmer). Following overnight culturing, cells were incubated for 6 hours with BrdUrd containing medium. After fixation for 1 hour, cells were stained for 1.5 hours with the peroxidase-conjugated anti-BrdUrd antibody, chemiluminescence substrate added and the emitted light quantified with a Centro LB 960 luminometer (Berthold Technologies GmbH).

For MTT assays, 20,000 to 25,000 cells were reseeded 24 hours after transfection in 24-well cell culture plates. After additional culturing for 24 or 48 hours, supernatant was replaced by MTT-containing medium (thiazolyl blue, Carl Roth GmbH) and plates were incubated for 2 hours at 37°C. Medium was replaced by solubilization solution (10% Triton-100, 0.1 mol/L hydrochloric acid in 2-propanol). Extinction was measured at 570 nm with the Multiskan FC photometer (Thermo Scientific).

Flow cytometric analysis

Forty-eight hours after transfection with siRNAs, cells were either left untreated or incubated with 0.1 μg/mL nocodazole for the indicated time periods. Cells were then trypsinized and centrifuged at 1,200 rpm for 3 minutes. After washing with PBS, pellets were thoroughly resuspended in 50–100 μL PBS and the

cell suspension transferred drop-wise into ice-cold ethanol (70%) under continuous vortexing. Following centrifugation at 1,000 g for 5 minutes, the supernatant was carefully discarded, the pellet washed with 500 μL ice-cold PBS and resuspended in 500 μL of propidium-iodide mixture (1 mg/mL propidium-iodide (Sigma-Aldrich) + 500 μg/mL DNAse-free RNAse (Roche Diagnostics) in PBS). Samples were incubated for 30 to 45 minutes at room temperature in the dark and subsequently measured with the flow cytometer LSR II (BD Biosciences). For data evaluation, the software FlowJo ver. 7.6.5 (Tree Star Inc.) was used.

RNA-Seq and pathway enrichment analyses

The quality and quantity of total RNA was measured using the RNA 6000 Nano chip on the 2100 BioAnalyzer (Agilent Technologies). Fifty nanograms of total RNA was converted to cDNA using the Ovation RNA-Seq System V2 (Nugen Technologies, Inc.) according to the manufacturer's protocol. This cDNA was used to construct libraries for massively parallel sequencing using Ovation Rapid DR Multiplex System 1-96 (Nugen Technologies, Inc.) according to the manufacturer's protocol. Massively parallel sequencing was performed on the HiSeq 2500 (Illumina Inc.) with paired-end sequencing, 100 bp read length, and at least 34 million read pairs per sample.

Three independent series of experiments were performed in which S2-007 cells were transfected with nonsilencing control siRNA or PLAC8-specific siRNAs 1, 2, or 3, respectively. Transcript counts were normalized for each individual sample and differentially expressed transcripts identified by comparing results from control-transfected cells versus cells transfected with all three PLAC8-specific siRNAs using the DESeq package (30). Statistical significance was determined based on negative binomial distribution, with variance and mean linked by local regression.

For pathway enrichment analyses, gene-pathway-association datasets were extracted from the Pathway Commons database (www.pathwaycommons.org). For the set of differentially expressed transcripts, the number of genes associated to a specific pathway was compared with the number of associations with this pathway among all known human transcripts in the database. Statistical significance was determined using the Fisher exact test adjusted for multiple testing by limiting the false discovery rate (FDR < 0.05).

Animal experiments

Animals were maintained in a climate-controlled room kept at 22°C, exposed to a 12:12-hour light-dark cycle, fed standard laboratory chow, and given water *ad libitum*.

The *Plac8*$^{-/-}$ mouse strain (6) as well as the *LsL-Kras*^{G12D}*; Pdx1-Cre* double mutant and *LsL-Kras*^{G12D}*;LsL-Trp53*^{R172H}*;Pdx1-Cre* triple mutant strains have been described previously (31). All mouse strains were originally on a mixed 129/SvJ/C57Bl/6 background but were backcrossed to a pure C57Bl/6 background for at least six generations. Mutant strains were intercrossed to produce cohorts with the genotypes indicated in the manuscript.

Upon signs of terminal illness, such as weight loss, diminished activity, and/or abdominal bloating due to ascites, mice were euthanized and the pancreas was removed, inspected for grossly visible tumors and preserved in 10% formalin solution (Sigma-Aldrich). Formalin-fixed, paraffin-embedded tissues were sectioned (4 μm), stained with hematoxylin and eosin, and histologically evaluated by an experienced gastrointestinal pathologist (B. Sipos) blinded to the experimental groups.

To compute and compare survival rates between mouse cohorts and generate Kaplan–Meier curves, the GraphPad Prism 5 program was used. All animals that were found to have invasive adenocarcinomas of the pancreas upon necropsy were included as events. Animals that died of other causes, as determined by histologic evaluation of pancreata after necropsy, as well as animals that were still alive at the time of evaluation were censored. Statistical significance was determined using the Log-rank (Mantel–Cox) test. A P value of <0.05 was considered significant.

Results

PLAC8 is strongly ectopically expressed in human PDAC

Our previous microarray analyses of microdissected human pancreatic tissues had indicated that *PLAC8* mRNA is expressed in high-grade preneoplastic lesions and invasive pancreatic carcinoma cells, whereas normal pancreata gave little or no signal (3). This was confirmed in qRT-PCR analyses, which showed that *PLAC8* mRNA is completely absent in normal human pancreas and most samples of inflamed pancreas (CP), whereas the majority of PDAC samples showed strong *PLAC8* mRNA expression (Fig. 1A). Interestingly, this pattern of ectopic *PLAC8* expression in transformed cells was faithfully mirrored in cultured cell lines. While immortalized, but nontransformed cells showed little or no detectable *PLAC8* expression, mRNA levels were moderate or high in five out of six pancreatic cancer cell lines analyzed (Fig. 1B).

These results were confirmed on the protein level using immunohistochemical staining of TMAs comprising 62 individual samples of PDAC as well as 60 chronically inflamed and 65 donor-derived healthy control tissues. PLAC8 staining was completely absent in healthy tissues, including areas of normal pancreas parenchyma adjacent to tumor lesions, as well as in inflamed tissues from CP patients. Staining frequency and intensity increased with increasing grades of preneoplastic lesions (PanINs), and in 38 out of 61 (62%) invasive carcinoma samples, tumor cells stained clearly positive for PLAC8 protein, showing apical and, to a lesser extent, cytoplasmic signal (Fig. 1C and D). Grade 2 and grade 3 PDAC showed higher PLAC8 expression compared with well differentiated tumors; however this tendency did not reach statistical significance (χ^2, $P = 0.059$). Log-rank analysis revealed no differences in survival of patients when stratified by no/weak versus moderate/strong PLAC8 expression ($P = 0.11$).

PLAC8 is localized at the inner face of the plasma membrane and stably interacts with defined membrane structures

We next sought to investigate the details of the subcellular localization of PLAC8 protein in the cancer cells. Immunofluorescence (IF) analyses of pancreatic cancer cells using a PLAC8-specific antibody demonstrated a prominent signal at the plasma membrane, with spotted staining of intracellular vesicular structures (Fig. 2A). Comparison of staining results with and without permeabilization of the plasma membrane strongly suggested that PLAC8 is localized on the inside of the plasma membrane, because the protein was not accessible to the antibody without permeabilization (Fig. 2B). These results were confirmed using fluorescence protein-tagged PLAC8 fusion proteins, which showed identical localization compared with IF staining of endogenous PLAC8 and were only accessible to anti-GFP antibodies following permeabilization of the plasma membrane

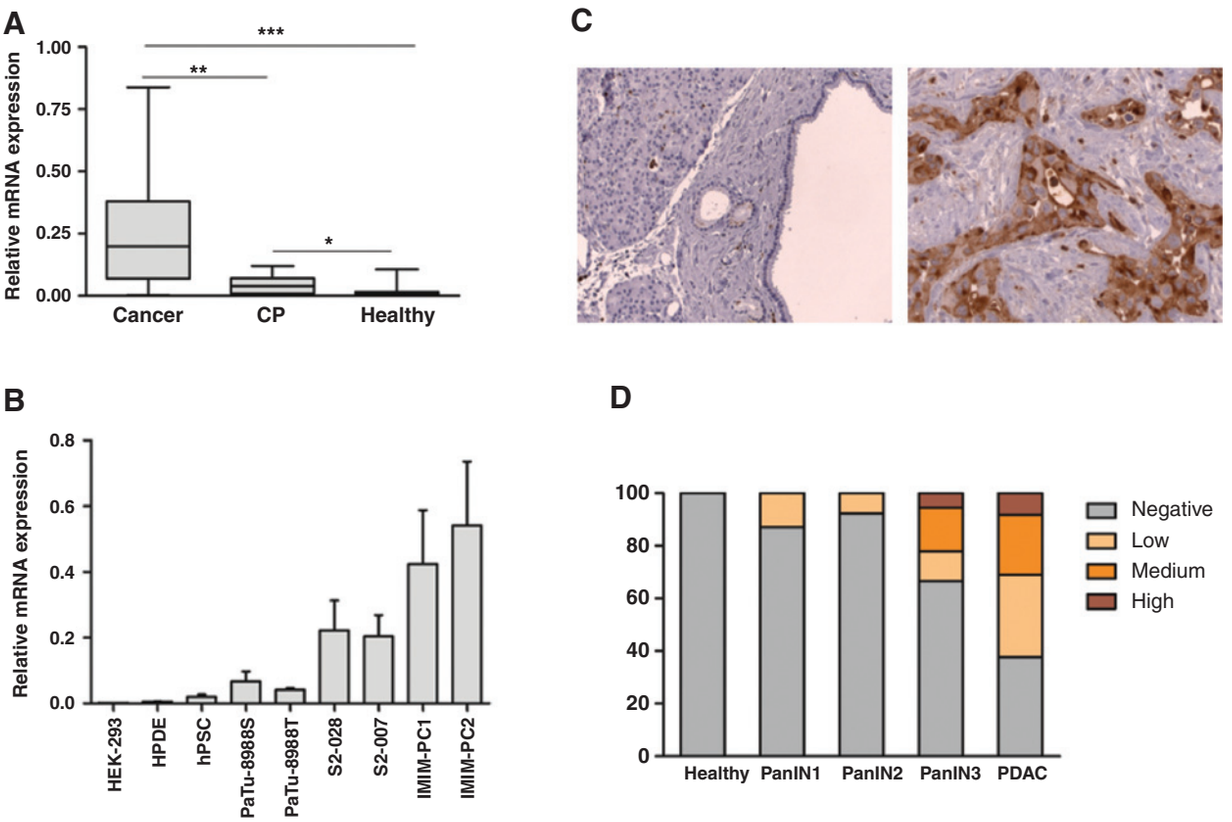

Figure 1.
PLAC8 is strongly ectopically expressed in PDAC. A, box-and-whisker plot showing *PLAC8* mRNA expression in primary human pancreatic tumor tissue samples, CP and normal pancreas as analyzed by qRT-PCR. Expression was normalized to ribosomal protein, large, P0 (RPLP0) mRNA levels. Data in figure represent median and second and third quartiles (boxes) as well as minimum and maximum values (whiskers). $n = 22$ for cancer and $n = 12$ each for CP and healthy tissue samples. *, $P < 0.05$; **, $P < 0.01$; ***, $P < 0.001$; Mann–Whitney test. B, analysis of *PLAC8* mRNA expression levels (qRT-PCR) in a variety of different pancreatic cancer cell lines as well as nontransformed control cells (HEK-293 human embryonal kidney cells, HPDE immortalized human pancreatic duct cells, hPSC immortalized human pancreatic stellate cells). Expression was normalized to ribosomal protein, large, P0 (RPLP0) mRNA levels. Experiments were performed in triplicates; bars represent mean expression values ± SEM. C, immunohistological analyses of PLAC8 expression using human pancreatic TMAs comprising 65 donor and 62 tumor tissues. PLAC8 protein was completely absent from healthy tissues (left plot; original magnification, ×100), whereas the majority of tumor cells in invasive PDAC stained positive (right plot; original magnification, ×630). Positive cells showed an apical and, to a lesser extent, cytoplasmic staining pattern, while nuclei were devoid of signal. D, PLAC8 staining frequency and intensity in individual ducts and lesions was quantitatively evaluated (Remmele immunoreactivity score). Scores significantly increased with the progression to advanced preneoplastic lesions (PanIN3) and invasive PDAC.

(Fig. 2C). Moreover, quantification of YFP-PLAC8 signals at different cellular localizations revealed 4-fold higher PLAC8 signal intensities at the membrane as compared with the cytosol of pancreatic cancer cells (Supplementary Fig. S1). Fluorescence protease protection assays in living pancreatic cancer cells demonstrated that intensity and localization of PLAC8-CFP fluorescence remained unchanged after plasma membrane permeabilization with digitonin under conditions where freely diffusible cytosolic YFP showed nearly complete loss of signal from the same cells (Fig. 2D, top and middle; see also Movie S1 in Supplementary Data at http://www.staff.uni-marburg.de/~buchhol3/Plac8/). PLAC8-CFP fluorescence was, however, sensitive to treatment of the permeabilized cells with trypsin (Fig. 2D, bottom), indicating that PLAC8 is located as an exposed protein at the inner face of the membrane under physiologic conditions.

Analysis of cells coexpressing PLAC8 and the GPI-anchored outer membrane protein PRNP showed that the PLAC8-positive vesicles frequently carried PRNP on the luminal side of the vesicles (Supplementary Fig. S2; Movie S2 in Supplementary Information). PrP is known to be transported to the cell surface via the secretory pathway. However, coexpression of PLAC8 with the ER marker ssRFPKDEK demonstrated that PLAC8 does not colocalize with any ER structures, neither in the absence (Fig. 3A) nor in the presence of brefeldin A (data not shown). Together, these results indicate that PLAC8-positive vesicles form by endocytotic processes at the plasma membrane rather than originating directly from the ER/Golgi system.

In FRAP experiments, PLAC8 showed intermediate local mobility, with recovery of fluorescence in bleached membrane areas completed within a time frame of approx. 100 seconds (Fig. 3B; Supplementary Movie S3). FLIP analyses, however, demonstrated that movement of PLAC8 across greater distances along the plasma membrane is severely limited, because fluorescence intensities at sites distant to the area of repeated bleaching did not significantly decrease even after prolonged treatment (>15

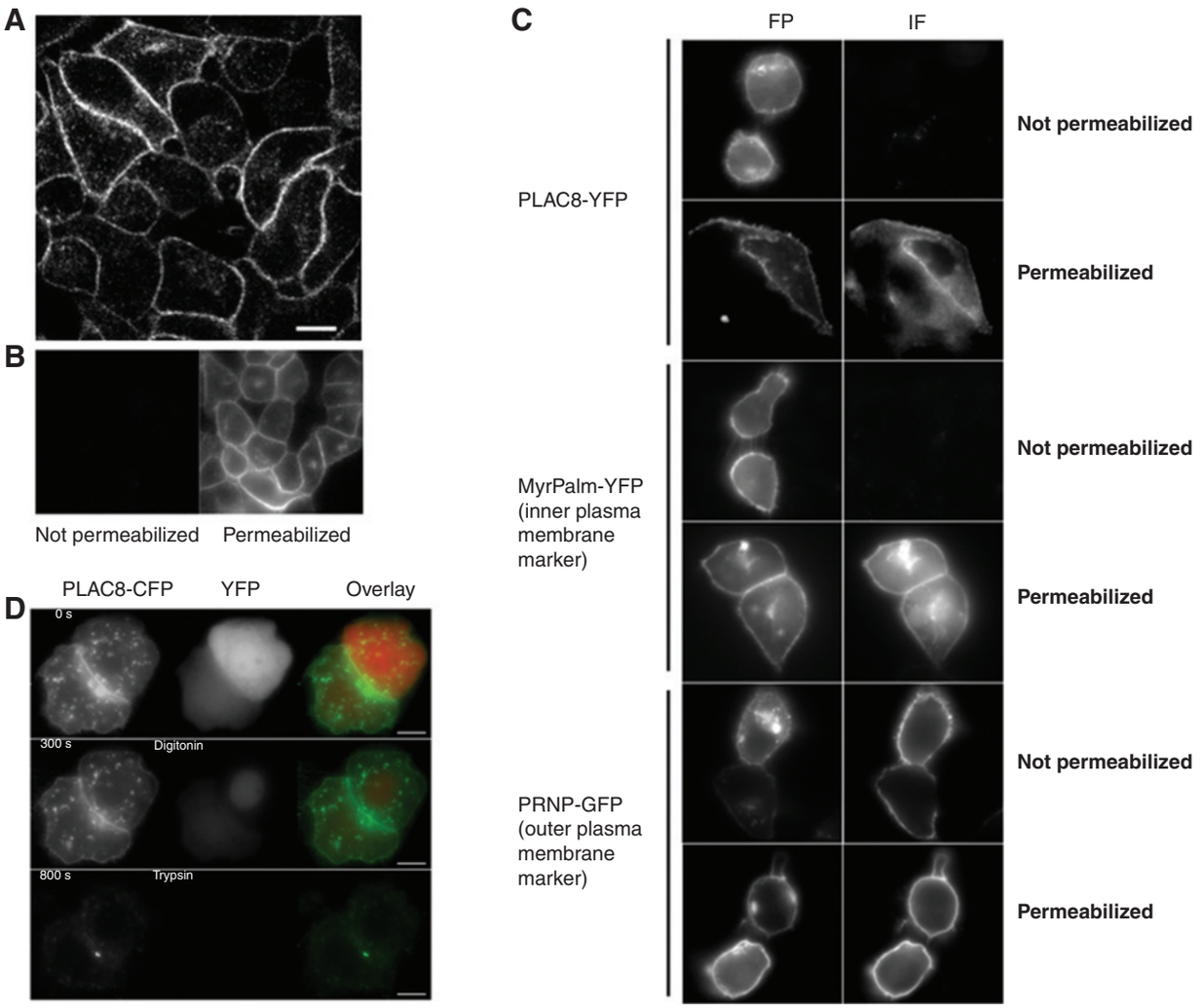

Figure 2.
PLAC8 localizes to the inner face of plasma membrane. A, fluorescent staining of endogenous PLAC8 in S2-007 pancreatic cancer cells. B, comparison of staining results with (right) and without (left) permeabilization of plasma membranes. C, S2-007 cells were transfected with PLAC8-YFP, MyrPalm-mEYFP, or PRNP-GFP fusion constructs and either analyzed for YFP/GFP fluorescence (left column of plots) or IF with anti-GFP antibodies (right column). Prior to fluorescence analyses, plasma membranes were permeabilized or not permeabilized as indicated. Similar to the inner plasma membrane marker MyrPalm-mEYFP, PLAC8-YFP was only accessible to anti-GFP antibodies after permeabilization. D, S2-007 cells were cotransfected with PLAC8-CFP (left; green pseudocolor in overlay) and YFP (middle; red pseudocolor in overlay) and fluorescence signals recorded before treatment (top) as well as after sequential treatment with digitonin (middle) and trypsin (bottom). Scale bars, 10 μm.

minutes), whereas fluorescence of freely diffusible cytosolic YFP was nearly completely abolished within the same time frame (Fig. 3C; Supplementary Movie S4). PLAC8 thus seems to tightly interact with stable and relatively immobile membrane structures. This is also supported by the results of TIRF microscopy experiments, which demonstrated that PLAC8 is not evenly distributed across the cell surface but is localized in defined structures that are very stable over the time frame of the analyses (10 minutes; Supplementary Movie S5).

Loss of PLAC8 expression severely impairs cell growth

To investigate the functional significance of PLAC8 expression in pancreatic cancer cells, we transiently silenced PLAC8 expression in two cell lines with high (S2-007) and intermediate (PaTu-8988T) PLAC8 expression levels using three independent siRNAs. Transfection of any of the siRNAs in both cell lines led to strong and highly significant reductions in the numbers of viable cells after 72 hours of incubation (Fig. 4A, top). Moreover, BrdUrd incorporation assays as a direct measure of DNA synthesis demonstrated that proliferative activity of the cells was profoundly attenuated following PLAC8 knockdown. This effect was again significant for all three siRNAs in both cell lines, although most pronounced for siRNA1 (Fig. 4A, middle). Western blot analyses for cleavage of PARP or caspase-3 proteins revealed no indication of enhanced apoptosis rates in PLAC8 knockdown cells (Fig. 4B), again suggesting that the growth inhibitory effects were primarily due to a decrease in proliferation rather than an increase in cell death. Surprisingly, though, flow cytometric analyses of PLAC8

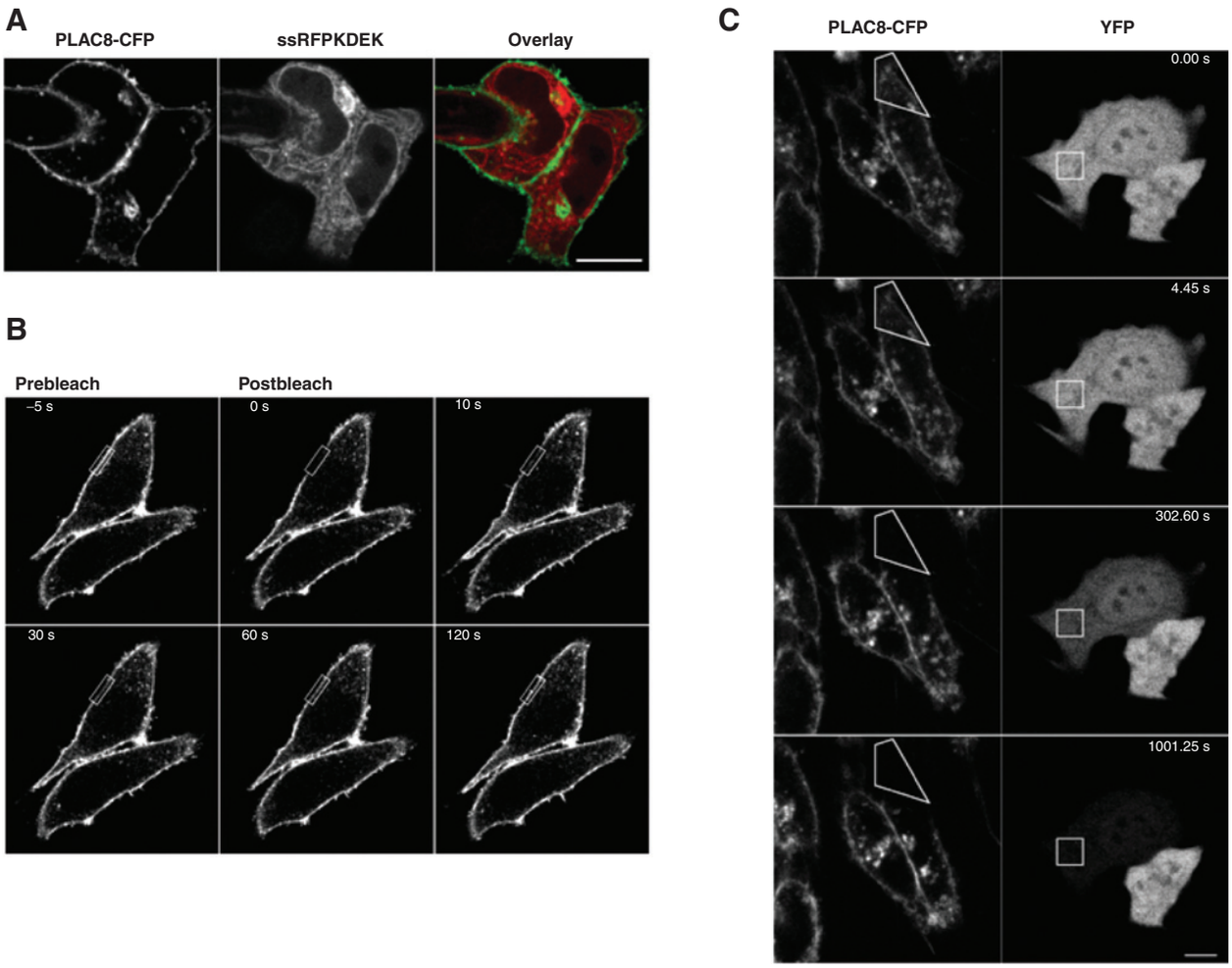

Figure 3.
PLAC8 stably interacts with defined membrane structures. A, S2-007 cells were cotransfected with PLAC8-CFP (left; green pseudocolor in overlay) and the ER marker ssRFPKDEK (middle; red pseudocolor in overlay). B, example of FRAP analysis. In a PLAC8-YFP-transfected S2-007 cell, a ROI covering a PLAC8-positive membrane area (white rectangle) was photobleached using high-power laser intensities. Recovery of fluorescence in the ROI was recorded and quantified over 120 seconds. The images before (prebleach) and immediately after (postbleach) the photobleaching, and at timepoints 10, 30, 60, and 120 seconds are shown. Scale bars, 10 μm. C, FLIP analysis. S2-007 cells were transfected with PLAC8-CFP (left) or YFP (right). ROIs (white outlines) in individual cells were repeatedly photobleached using high-power laser intensities and fluorescent signals recorded in regular intervals for up to 20 minutes of total duration.

knockdown and control cells in the absence of additional treatment showed no overt changes in the proportion of cells in different phases of the cell cycle, with the exception of siRNA1, which produced evidence of a G_1–S arrest. However, incubation of the cells with the cell-cycle inhibitor nocodazole, which arrests cells in G_2–M phase and thus prevents individual cells from reentering the cell cycle, revealed that all three siRNAs profoundly attenuated cell-cycle progression. While this inhibitory effect was more evenly distributed across all phases of the cycle for cells transfected with siRNAs 2 and 3, as evidenced by the slower depletion of cells from G_1, slower accumulation of cells in G_2 and essentially unchanged proportion of cells in S-phase, cells transfected with siRNA1 remained arrested in G_1 (Fig. 4C; Supplementary Fig. S3). It is thus likely that siRNA1 induced off-target effects in addition to the specific effects of PLAC8 depletion, resulting in a complete block of G_1–S transition.

PLAC8 knockdown affects central regulators of cell growth

To gain insights into the molecular mechanisms that mediate the functional effects of PLAC8 knockdown in the cancer cells, we performed proteomic analyses of PLAC8 knockdown and control cells using RPPA technology (32). Whole cell lysates were probed with a total of 207 well-characterized antibodies examining expression levels and/or phosphorylation status of central regulators of cell growth or constituents of major signaling pathways. The results of these analyses are summarized in Supplementary Table S1; all raw data can be accessed at http://www.staff.uni-marburg.de/~buchhol3/Plac8/.

Two of the most striking results were the uniform decrease in levels of phosphorylated retinoblastoma protein (RB1-P-$Ser^{807/811}$) as well as phosphorylated ribosomal protein S6 (RPS6-P-$Ser^{235/236}$) in PLAC8 knockdown cells (Fig. 5A), both of which are well known to be central regulators of cell growth

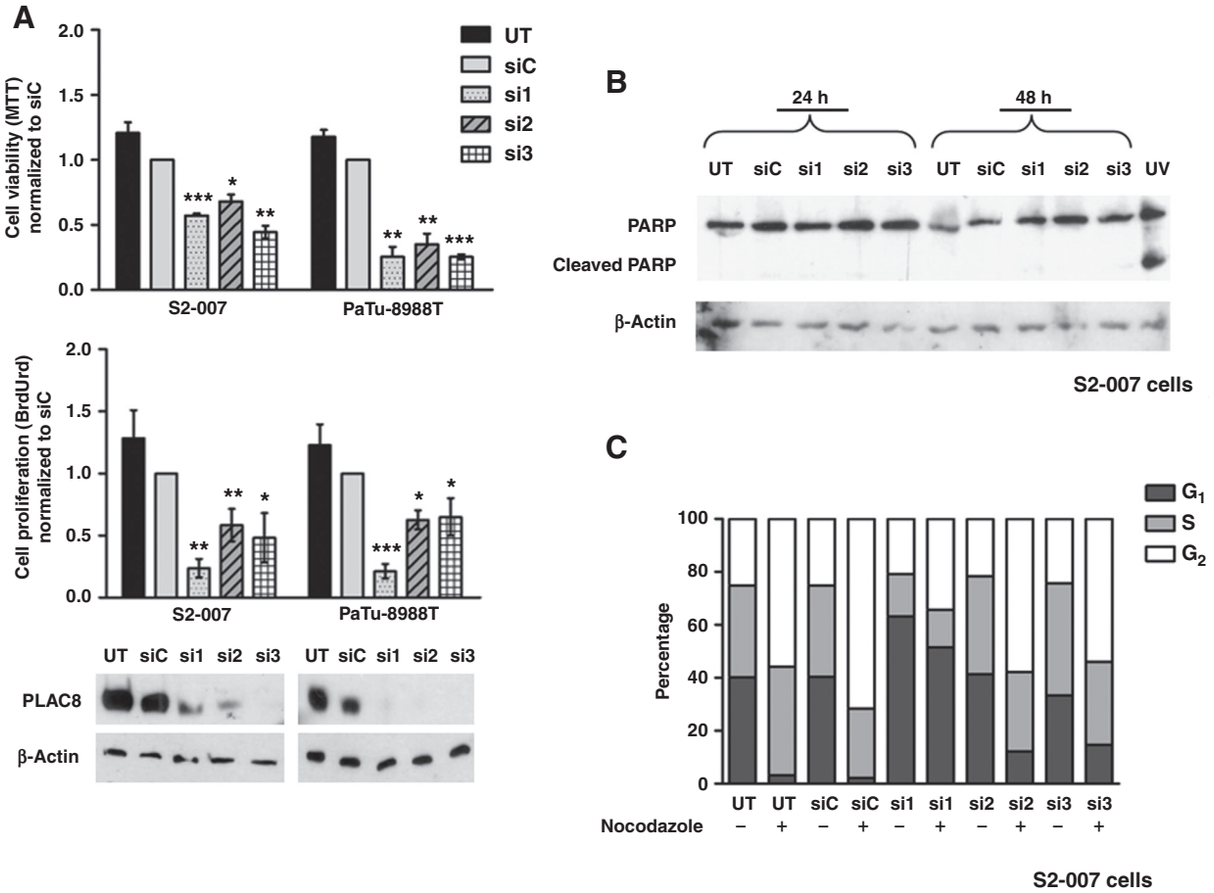

Figure 4.
RNAi-mediated loss of PLAC8 expression severely impairs pancreatic cancer cell growth. A, PLAC8 expression in S2-007 and PaTu-8988T cells was inhibited using three independent *PLAC8*-specific siRNAs, leading to strong reduction of PLAC8 protein levels in both cell lines (bottom, Western blots). PLAC8 loss significantly impaired viability and proliferation of pancreatic cancer cell lines as assessed by MTT (top) and DNA BrdUrd incorporation (middle) assays, respectively. Bars represent mean ± SEM of at least three independent experiments normalized to siC. si1–si3, PLAC8-specific siRNAs; siC, nonsilencing control siRNA; UT, untreated cells. *, $P < 0.05$; **, $P < 0.01$; ***, $P < 0.001$ (Student *t* test). B, Western blot analyses revealed no indication of increased levels of cleaved PARP protein 24 or 48 hours after transfection of siRNAs. UV, cells treated with UV light (positive control). C, 48 hours after transfection with siRNAs, cells were either left untreated or incubated with 0.1 μg/mL nocodazole for 9 hours and cell-cycle distribution analyzed by flow cytometry. While both G_1–S and S/G2 transition were attenuated in cells treated with siRNAs 2 and 3, cells were completely arrested in G_1 after transfection with siRNA1.

(cell cycle) and proliferation, whereas no antiproliferative effects in the Ras-Raf-Erk pathway were detected. Western blot analyses of cell lysates from PLAC8 knockdown and control cells confirmed these posttranslational changes (Fig. 5B), whereas total levels of both proteins remained unchanged (data not shown). Moreover, the tumor suppressor p21, which acts upstream of RB1, was strongly upregulated following PLAC8 knockdown (Fig. 5B), providing a further hint at the regulatory events mediating the inhibition of cell-cycle progression. Although previous publications had indicated a functional link between PLAC8 and the MYC oncogene as well as a direct interaction of PLAC8 with AKT1 in myeloid and fibroblast cells, respectively (10), PLAC8 knockdown experiments revealed no such interactions in pancreatic cancer cells, indicating that these interactions may be cell type specific (Supplementary Fig. S4).

To additionally characterize transcriptional changes within the cells following PLAC8 knockdown, we performed global transcriptome analyses of PLAC8 knockdown and control cells using next generation sequencing techniques (RNA-Seq). FDR-controlled comparison of S2-007 cells with PLAC8 knockdown and control-treated cells identified a total of 92 transcripts that were significantly changed in cells treated with siRNAs against PLAC8 as compared with cells treated with nonsilencing control siRNA (Supplementary Table S2; Supplementary Fig. S5). Among others, PLAC8 knockdown caused a significant downregulation of cyclin D1 mRNA, which also translated into significant downregulation of cyclin D1 protein (Fig. 5B). Moreover, pathway enrichment analyses based on the RNA-Seq results showed that multiple surface receptor pathways, including multiple instances of PI3 kinase/Akt/mTor pathways, were significantly impacted by the PLAC8 knockdown (Supplementary Table S3).

In contrast, neither Western blot analyses of isoform ratios of the autophagy indicator LC3 (Fig. 5D) nor gene set enrichment analyses of RNA-seq data provided any indication of changes in autophagy-related mechanisms in response to altered PLAC8 expression levels.

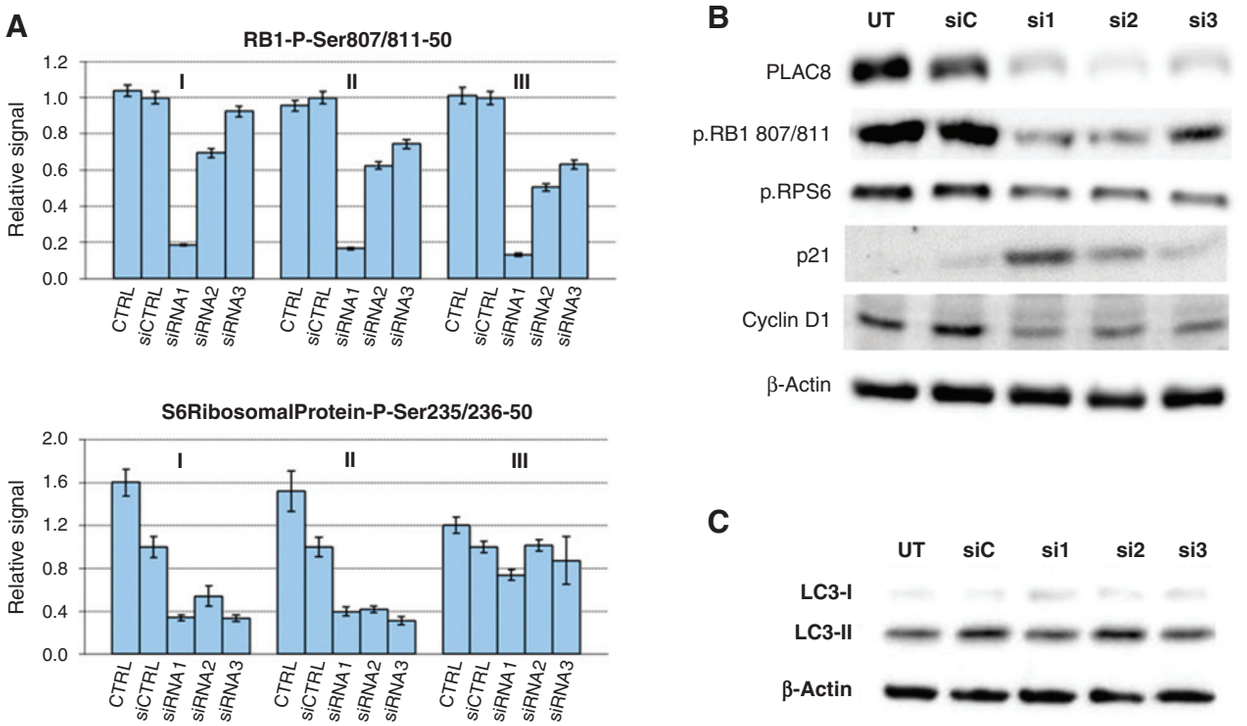

Figure 5.
PLAC8 knockdown affects central regulators of cell growth. A, RPPA analyses revealed significant reduction in the levels of phosphorylated retinoblastoma protein (RB1-P-Ser807/811; top) and phosphorylated ribosomal protein S6 (RPS6-P-Ser235/236; bottom) in S2-007 cells transfected with PLAC8-specific siRNAs. Three independent experiments were performed. B, immunoblotting of selected cell-cycle regulators in S2-007 cells with and without PLAC8 knockdown. UT, untreated cells; siC, nonsilencing control siRNA; si1-si3, *PLAC8*-specific siRNAs. C, immunoblotting of LC3 protein (autophagy indicator) from S2-007 cells with and without PLAC8 knockdown revealed no changes in the relative abundance of LC3 isoforms.

Plac8 deficiency attenuates tumor progression in a Kras–driven, but not a Kras/Trp53–driven mouse model of pancreatic cancer

In order to evaluate the functional significance of Plac8 expression for pancreatic tumorigenesis *in vivo*, we analyzed the well-established the *LsL-Kras*^{G12D}*; Pdx1-Cre* ("KC") and *LsL-Kras*^{G12D}*; LsL-Trp53*^{R172H}*;Pdx1-Cre* ("KPC") pancreatic cancer models (31). qRT-PCR analyses demonstrated that in striking analogy to the human situation, murine Plac8 was strongly upregulated in malignant cells from tumors forming in KC and KPC mice, while healthy pancreata were devoid of Plac8 expression (Fig. 6A). Interestingly, both immortalized EpH4 mouse mammary epithelial cells as well as their Hras-transformed counterparts (EpRas; 33) were likewise Plac8-negative (Fig. 6A, right lanes), indicating that Ras-driven malignant transformation of epithelial cells in and of itself does not necessarily cause ectopic Plac8 expression.

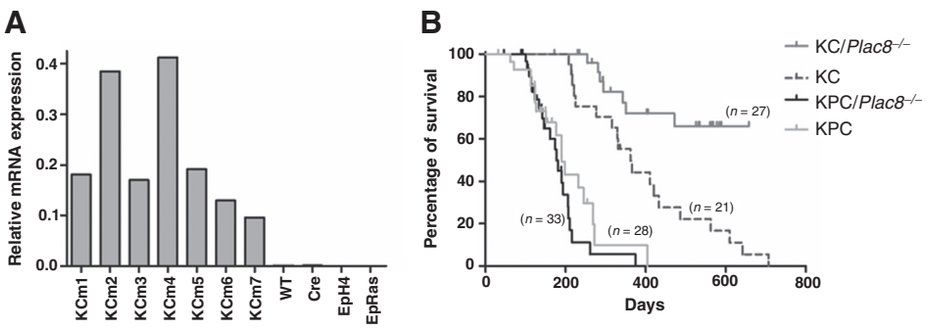

Figure 6.
Plac8 deficiency attenuates tumor progression in a KRAS-driven PDAC mouse model. A, *Plac8* mRNA expression (qRT-PCR) was assessed in cell lines established from tumors from *LsL-Kras*^{G12D}*; Pdx1-Cre* double mutant (KC) mice as well as in pancreata from wild-type (WT) and *Pdx1-Cre* (Cre) control mice and in the EpH4/EpRas cell line system. Expression levels were normalized to ribosomal protein, large, P0 (Rplp0) mRNA levels. B, Kaplan–Meier analyses revealed that Plac8 deficiency did not result in any survival benefit in the KPC mouse model ($P = 0.182$, Log-rank test), whereas survival of KC mice on *Plac8* knockout background was significantly prolonged compared with KC mice with wild-type Plac8 ($P = 0.0022$, Log-rank test).

We next crossed KC and KPC mice with mice harboring a global *Plac8* gene knockout (*Plac8*$^{-/-}$ mice) to determine the dependency of pancreatic tumor formation and progression on the ability to ectopically activate Plac8 expression in the pancreatic epithelial cells. Plac8 deficiency strongly attenuated tumor formation in KC mice, leading to significantly enhanced survival of KC/*Plac8*$^{-/-}$ mice compared with their Plac8-positive counterparts ($P = 0.0022$; Log-rank test; Fig. 6B). Median survival in the KC mouse cohort was 362 days, whereas median survival in the KC/*Plac8*$^{-/-}$ cohort was undetermined as more than 50% of mice were still alive at the time of analysis. Unexpectedly, though, Plac8 status had no influence on survival in the KPC mouse model, with median survival times of 190 days versus 177 days in the KPC versus the KPC/*Plac8*$^{-/-}$ cohorts, respectively (Fig. 6B).

Histopathologic evaluation of tumors from Plac8-deficient and Plac8-expressing KC and KPC mice did not reveal any systematic differences in tumor characteristics, such as cellular composition, differentiation etc.

Discussion

Subsequent to our initial identification of *PLAC8* as a PDAC-associated gene in whole-genome gene expression analyses of microdissected human tissues (3), a rapidly growing body of evidence had been accumulating suggesting that PLAC8 is an important player in many different cellular processes, and that its precise role varies greatly depending on the specific cellular context. Although PLAC8 overexpression protected rat fibroblasts from apoptosis (10), this effect was not observed in primary acute myeloid leukemia cells, where instead PLAC8 was reported to inhibit cell differentiation (12). Moreover, PLAC8 overexpression resulted in induction, rather than inhibition, of apoptosis in both primary and transformed human lymphocytes (11), and decreased PLAC8 expression was reported to be associated with oncogenesis in the liver (34). Further evidence for context-dependent differential roles of PLAC8 comes from a study by Li and colleagues (13), who demonstrated that PLAC8 overexpression caused decreased migration of mesenchymal cells in zebrafish embryos, while resulting in enhanced migration and features reminiscent of epithelial-to-mesenchymal transition in cultured colon cancer cells.

Our own results add yet another facet to the astonishing versatility of cellular functions that this protein fulfills. We demonstrate that ectopic expression of PLAC8 protein in the epithelial cancer cells is a regular feature of the majority of human PDAC tumors, and that PLAC8 upregulation is a late event in the transformation of pancreatic epithelial cells, as evidenced by the virtually complete lack of PLAC8 in early PanIN lesions and the sharp rise in PLAC8 positivity from PanIN3 to invasive PDAC lesions. This is also the first study to provide a detailed view of the subcellular distribution of PLAC8 protein in pancreatic cancer cells. The apical staining pattern in primary human PDAC tissues already hinted at a membranous localization of PLAC8 in PDAC cells. This was unequivocally confirmed by immunocytological analyses of a wide range of pancreatic cancer cell lines (shown for S2-007 and PaTu-8988T cells in this study), and further corroborated by identical localization of fluorescence-tagged recombinant PLAC8 expression constructs.

Functional confocal microscopy analyses of living pancreatic cancer cells, including FLIP-, FRAP-, and TIRF assays, demonstrated that PLAC8 is not uniformly distributed across the cell surface, but stably interacts with specific structures at the inner face of the plasma membrane. It will be of great interest to identify the interaction partner(s) that mediate this distinct localization pattern, thereby potentially also providing new clues about the still-enigmatic molecular function(s) of PLAC8. Using yeast two hybrid screening techniques, Li and colleagues (35) have previously identified phospholipid scramblase1 (PLSCR1) as an interaction partner of PLAC8 in Cos7 cells as well as NIH 3T3 and Rat1 fibroblasts, reporting an inhibitory interaction between the two proteins and a proapoptotic effect of PLSCR1 expression in the absence of PLAC8. Being a ubiquitously expressed endofacial membrane protein, PLSCR1 would also be a potential interaction partner in pancreatic cancer cells. However, PLSCR1 knockdown in pancreatic cancer cells inhibited, rather than promoted, cell growth in pancreatic cancer cell lines (data not shown), and deletion of the cysteine-rich domain of PLAC8 (aa28 to 38), which was reported by Li and colleagues to inhibit the interaction between PLSCR1 and PLAC8, did not prevent membrane localization of PLAC8 in pancreatic cancer cells (data not shown). Moreover, apoptosis levels were not altered in pancreatic cancer cells in response to PLAC8 inhibition, suggesting that the effects observed by Li and colleagues are again strongly context-dependent.

A recent report by Kinsey and colleagues (36) suggested that PLAC8 expression promotes tumor progression in epithelial tumors (including pancreatic cancer) via autophagy-related mechanisms. Our own results, however, clearly exclude autophagy-related functions of PLAC8 in pancreatic cancer cells. Instead, high-throughput proteomic and transcriptomic analyses as well as flow cytometric and immunoblotting analyses identified a distinct effect of PLAC8 downregulation on cell-cycle progression in pancreatic cancer cells, which was not reported in other cell systems before. These discrepancies again most probably stem from the choice of experimental cell systems that were used. For the majority of their functional analyses, Kinsey and colleagues used mouse colon epithelial cells that were artificially transformed by mutational Kras activation and Trp53 inhibition. In contrast to healthy pancreas tissue, which is completely devoid of PLAC8 protein, colon epithelia physiologically show PLAC8 expression at the apical domain of colonocytes and goblet cells (13). Interestingly, loss of epithelial PLAC8 expression was observed in ca. 50% of colorectal cancer cases, whereas 11% of cases showed strong cytoplasmic PLAC8 staining, which correlated with higher tumor grade and microsatellite instability (13). The lysosomal localization and autophagy-related function of PLAC8 observed by Kinsey and colleagues can thus be speculated to be a distinct feature of a subset of colon cancer cells.

In similarity to the results of Kinsey and colleagues, however, Plac8 deficiency caused differential effects in GEMMS of pancreatic cancer. Their study included the analysis of GEMMs in which the formation of pancreatic tumors was induced by pancreas-specific activation of oncogenically mutated Kras and concordant deletion of the Trp53 tumor suppressor. Plac8 deficiency significantly prolonged survival in *Pdx1-Cre;LSL-Kras*^{G12D}*;p53*$^{L/+}$ mice, whereas no survival benefit was apparent in mice in which both *Trp53* alleles were deleted. In our own study, survival of *Plac8* knockout mice was significantly enhanced when tumorigenesis was induced by expression of oncogenic Kras alone, whereas survival was not impacted in

mice with concordant functional inactivation of Trp53 through conditional expression of a mutated allele (*Trp53*^{R172H}). These differential effects of Plac8 deficiency can be interpreted to again reflect the specific role of Plac8 expression during late phases of malignant transformation. In both sets of mouse models, the mutated alleles are activated in early embryonic stages of pancreatic development. Studies with alternative model systems, in which oncogenic mutations are activated in adult animals, have demonstrated that these mice are much more resistant to the genetic alterations, requiring additional stimuli such as induction of inflammation in the pancreas for tumorigenesis to occur (37, 38). These models are likely a much better representation of the human situation, highlighting the requirement for multiple oncogenic insults to induce tumor formation in the adult pancreas. It will thus be of great interest to study the impact of Plac8 deficiency on tumor formation in postnatal PDAC mouse models.

In summary, we demonstrate here that PLAC8 actively promotes PDAC development and progression by acting as a central regulator of Kras–driven tumorigenesis and directly affecting cell-cycle progression in pancreatic cancer cells *in vitro* and *in vivo*. Moreover, PLAC8 protein is completely absent from healthy or chronically inflamed pancreatic tissues, but is strongly ectopically expressed in the majority of human pancreatic cancers. Taken together, these results establish PLAC8 as an attractive new target for the development of novel diagnostic and therapeutic approaches in pancreatic cancer.

Disclosure of Potential Conflicts of Interest

No potential conflicts of interest were disclosed.

Disclaimer

This article reflects only the author's views and the European Union is not liable for any use that may be made of the information contained therein.

Authors' Contributions

Conception and design: B.P. Kaistha, T.M. Gress, M. Buchholz
Development of methodology: B.P. Kaistha, B. Sipos, S. Kelkenberg, T.M. Gress, M. Buchholz
Acquisition of data (provided animals, acquired and managed patients, provided facilities, etc.): B.P. Kaistha, H. Lorenz, B. Sipos, M. Pawlak, B. Gierke, R. Kreider, B. Lankat-Buttgereit, M. Sauer, L. Fiedler, A. Krattenmacher, B. Geisel, K.K. Frese, N.A. Giese
Analysis and interpretation of data (e.g., statistical analysis, biostatistics, computational analysis): B.P. Kaistha, H. Schmidt, B. Sipos, M. Pawlak, B. Geisel, J.M. Kraus, H.A. Kestler, T.M. Gress, M. Buchholz
Writing, review, and/or revision of the manuscript: B.P. Kaistha, B. Sipos, M. Pawlak, B. Lankat-Buttgereit, K.K. Frese, N.A. Giese, H.A. Kestler, T.M. Gress, M. Buchholz
Administrative, technical, or material support (i.e., reporting or organizing data, constructing databases): H. Lorenz, T.M. Gress
Study supervision: B.P. Kaistha, T.M. Gress, M. Buchholz
Other (microscopy image processing): H. Lorenz

Grant Support

This work was funded in part by the German Research Foundation (DFG; grant Bu 1536/3-1), Heidelberger Pancobank (BMBF grant 01GS08114), BMBF grant 01EY1101, and EU FP7 grant no. 602783 (large-scale integrated project "CAM-PaC").

The costs of publication of this article were defrayed in part by the payment of page charges. This article must therefore be hereby marked *advertisement* in accordance with 18 U.S.C. Section 1734 solely to indicate this fact.

Received January 21, 2015; revised August 18, 2015; accepted August 22, 2015; published OnlineFirst December 15, 2015.

References

1. Siegel R, Naishadham D, Jemal A. Cancer statistics, 2012. CA Cancer J Clin 2012;62:10–29.
2. Michl P, Gress TM. Current concepts and novel targets in advanced pancreatic cancer. Gut 2013;62:317–26.
3. Buchholz M, Braun M, Heidenblut A, Kestler HA, Kloppel G, Schmiegel W, et al. Transcriptome analysis of microdissected pancreatic intraepithelial neoplastic lesions. Oncogene 2005;24:6626–36.
4. Galaviz-Hernandez C, Stagg C, de RG, Tanaka TS, Ko MS, Schlessinger D, et al. Plac8 and Plac9, novel placental-enriched genes identified through microarray analysis. Gene 2003;309:81–9.
5. Tanaka TS, Jaradat SA, Lim MK, Kargul GJ, Wang X, Grahovac MJ, et al. Genome-wide expression profiling of mid-gestation placenta and embryo using a 15,000 mouse developmental cDNA microarray. Proc Natl Acad Sci U S A 2000;97:9127–32.
6. Ledford JG, Kovarova M, Koller BH. Impaired host defense in mice lacking ONZIN. J Immunol 2007;178:5132–43.
7. Jimenez-Preitner M, Berney X, Uldry M, Vitali A, Cinti S, Ledford JG, et al. Plac8 is an inducer of C/EBPbeta required for brown fat differentiation, thermoregulation, and control of body weight. Cell Metab 2011;14:658–70.
8. Jimenez-Preitner M, Berney X, Thorens B. Plac8 is required for white adipocyte differentiation in vitro and cell number control in vivo. PLoS One 2012;7:e48767.
9. Ledford JG, Kovarova M, Jania LA, Nguyen M, Koller BH. ONZIN deficiency attenuates contact hypersensitivity responses in mice. Immunol Cell Biol 2012;90:733–42.
10. Rogulski K, Li Y, Rothermund K, Pu L, Watkins S, Yi F, et al. Onzin, a c-Myc-repressed target, promotes survival and transformation by modulating the Akt-Mdm2-p53 pathway. Oncogene 2005;24:7524–41.
11. Mourtada-Maarabouni M, Watson D, Munir M, Farzaneh F, Williams GT. Apoptosis suppression by candidate oncogene PLAC8 is reversed in other cell types. Curr Cancer Drug Targets 2013;13:80–91.
12. Wu SF, Huang Y, Hou JK, Yuan TT, Zhou CX, Zhang J, et al. The down-regulation of onzin expression by PKCepsilon-ERK2 signaling and its potential role in AML cell differentiation. Leukemia 2010;24:544–51.
13. Li C, Ma H, Wang Y, Cao Z, Graves-Deal R, Powell AE, et al. Excess PLAC8 promotes an unconventional ERK2-dependent EMT in colon cancer. J Clin Invest 2014;124:2172–87.
14. Lieber M, Mazzetta J, Nelson-Rees W, Kaplan M, Todaro G. Establishment of a continuous tumor-cell line (panc-1) from a human carcinoma of the exocrine pancreas. Int J Cancer 1975;15:741–7.
15. Zur HH. Induction of specific chromosomal aberrations by adenovirus type 12 in human embryonic kidney cells. J Virol 1967;1:1174–85.
16. Iwamura T, Caffrey TC, Kitamura N, Yamanari H, Setoguchi T, Hollingsworth MA. P-selectin expression in a metastatic pancreatic tumor cell line (SUIT-2). Cancer Res 1997;57:1206–12.
17. Vila MR, Lloreta J, Schussler MH, Berrozpe G, Welt S, Real FX. New pancreas cancers cell lines that represent distinct stages of ductal differentiation. Lab Invest 1995;72:395–404.
18. Ouyang H, Mou L, Luk C, Liu N, Karaskova J, Squire J, et al. Immortal human pancreatic duct epithelial cell lines with near normal genotype and phenotype. Am J Pathol 2000;157:1623–31.
19. Simpson JC, Wellenreuther R, Poustka A, Pepperkok R, Wiemann S. Systematic subcellular localization of novel proteins identified by large-scale cDNA sequencing. EMBO Rep 2000;1:287–92.
20. Steigemann P, Wurzenberger C, Schmitz MH, Held M, Guizetti J, Maar S, et al. Aurora B-mediated abscission checkpoint protects against tetraploidization. Cell 2009;136:473–84.
21. Lorenz H, Windl O, Kretzschmar HA. Cellular phenotyping of secretory and nuclear prion proteins associated with inherited prion diseases. J Biol Chem 2002;277:8508–16.
22. Kim PK, Mullen RT, Schumann U, Lippincott-Schwartz J. The origin and maintenance of mammalian peroxisomes involves a de novo PEX16-dependent pathway from the ER. J Cell Biol 2006;173:521–32.

23. Chakrabarti O, Hegde RS. Functional depletion of mahogunin by cytosolically exposed prion protein contributes to neurodegeneration. Cell 2009;137:1136–47.
24. Lorenz H, Hailey DW, Wunder C, Lippincott-Schwartz J. The fluorescence protease protection (FPP) assay to determine protein localization and membrane topology. Nat Protoc 2006;1:276–9.
25. Lorenz H, Hailey DW, Lippincott-Schwartz J. Fluorescence protease protection of GFP chimeras to reveal protein topology and subcellular localization. Nat Methods 2006;3:205–10.
26. Lippincott-Schwartz J, Snapp E, Kenworthy A. Studying protein dynamics in living cells. Nat Rev Mol Cell Biol 2001;2:444–56.
27. Ellenberg J, Siggia ED, Moreira JE, Smith CL, Presley JF, Worman HJ, et al. Nuclear membrane dynamics and reassembly in living cells: targeting of an inner nuclear membrane protein in interphase and mitosis. J Cell Biol 1997;138:1193–206.
28. Schneider CA, Rasband WS, Eliceiri KW. NIH Image to ImageJ: 25 years of image analysis. Nat Methods 2012;9:671–5.
29. Pirnia F, Pawlak M, Thallinger GG, Gierke B, Templin MF, Kappeler A, et al. Novel functional profiling approach combining reverse phase protein microarrays and human 3-D ex vivo tissue cultures: expression of apoptosis-related proteins in human colon cancer. Proteomics 2009; 9:3535–48.
30. Anders S, Huber W. Differential expression analysis for sequence count data. Genome Biol 2010;11:R106-R111.
31. Hingorani SR, Wang L, Multani AS, Combs C, Deramaudt TB, Hruban RH, et al. Trp53R172H and KrasG12D cooperate to promote chromosomal instability and widely metastatic pancreatic ductal adenocarcinoma in mice. Cancer Cell 2005;7:469–83.
32. Akbani R, Becker KF, Carragher N, Goldstein T, De KL, Korf U, et al. Realizing the promise of reverse phase protein arrays for clinical, translational, and basic research: a workshop report: the RPPA (Reverse Phase Protein Array) society. Mol Cell Proteomics 2014;13:1625–43.
33. Janda E, Lehmann K, Killisch I, Jechlinger M, Herzig M, Downward J, et al. Ras and TGF[beta] cooperatively regulate epithelial cell plasticity and metastasis: dissection of Ras signaling pathways. J Cell Biol 2002;156:299–313.
34. Grate LR. Many accurate small-discriminatory feature subsets exist in microarray transcript data: biomarker discovery. BMC Bioinformatics 2005;6:97.
35. Li Y, Rogulski K, Zhou Q, Sims PJ, Prochownik EV. The negative c-Myc target onzin affects proliferation and apoptosis via its obligate interaction with phospholipid scramblase 1. Mol Cell Biol 2006;26:3401–13.
36. Kinsey C, Balakrishnan V, O'Dell MR, Huang JL, Newman L, Whitney-Miller CL, et al. Plac8 links oncogenic mutations to regulation of autophagy and is critical to pancreatic cancer progression. Cell Rep 2014;7:1143–55.
37. Guerra C, Schuhmacher AJ, Canamero M, Grippo PJ, Verdaguer L, Perez-Gallego L, et al. Chronic pancreatitis is essential for induction of pancreatic ductal adenocarcinoma by K-Ras oncogenes in adult mice. Cancer Cell 2007;11:291–302.
38. Guerra C, Collado M, Navas C, Schuhmacher AJ, Hernandez-Porras I, Canamero M, et al. Pancreatitis-induced inflammation contributes to pancreatic cancer by inhibiting oncogene-induced senescence. Cancer Cell 2011;19:728–39.